

Electrochemical Impedance Studies on Tribocorrosion of Coatings $\text{Al}_x\text{Ti}_{1-x}\text{N}$ Deposited on Austenitic Steels

W. Aperador*, J. Duque, E. Delgado

School of Engineering, Universidad Militar Nueva Granada, Bogotá-Colombia

*E-mail: g.ing.materiales@gmail.com

Received: 19 November 2015 / Accepted: 9 December 2015 / Published: 1 January 2016

This paper presents the evaluation of properties tribocorrosion of the $\text{Al}_x\text{Ti}_{1-x}\text{N}$ multilayer, deposited on AISI 316L through the technique of physical vapor deposition magnetron sputtering. Corrosion tests were conducted, wear dry (without lubrication) and tribocorrosion tests (synergy between corrosion and wear) which they were carried out with a potentiostat and a pin-on-disk to which is was adapted to an electrochemical cell with three electrodes. The evaluation of the tests tribocorrosion it performed using the technique electrochemical impedance spectroscopy (EIS). The coefficient of friction depends on the mixture of titanium and aluminum, generating surfaces with better mechanical properties in a 60 Ti -40 Al mix, with respect to electrochemical system assisted by mechanical wear it corresponds the best system having higher content of titanium.

Keywords: tribocorrosion , thin film, $\text{Al}_x\text{Ti}_{1-x}\text{N}$, Austenitic Steels, Wear.

1. INTRODUCTION

The application of thin films to industry inferred control to the greatest extent possible the intrinsic variables the film growth and their effect on the coating characteristics, thanks to this great interest in the study of the growth of thin films and their effect on the characteristics and properties of the same is generated [1-3]. The growth of thin films is performed by nucleation processes, this process begins when the atoms are vaporized and sprayed from the target surface by physical means, to reach the substrate surface they are physically absorbed, because these particles are not in thermodynamic equilibrium with the substrate, they can interact with other species and mobility depends on the binding energy of the atoms to the substrate and the temperature thereof [4-5]; at higher temperature and lower mobility binding energy of the atoms, it is greater on the substrate surface and the possibility of conglomerated, clusters that are not thermodynamically stable will be absorbed by

the surface, on the contrary, thermodynamically stable clusters overcome the nucleation barrier and begin the process of growth, due to diffusion of atoms, nuclei growth at the substrate surface, occurs until the islands are large enough so that there is coalescence and the film begins to grow vertically, with the arrival of new species already sprayed [6-7].

Thus, the atoms may be located in a variety of spatial arrangements from randomly absorbed atoms, to perfect arrangements of films on arrangement of atoms; these types can be classified into three types of growth [8-9].

Thin films produced by Physical Vapor Deposition plasma assisted techniques (PAPVD), they have been widely used in mechanical and tribological applications to solve problems in surface engineering, because of the hardness, wear resistance, fatigue resistance and resistance in corrosive media, making them ideal for applications related to biocompatibility [10-12]. They also have a low density, and high melting point property which is often chosen for aircraft and automotive applications [13].

Corrosion wear is caused by prolonged use, and is a problem that must be addressed in a sector of the metalworking industry [14], because the causes of this erosion is a production imperfections in surface finish, thus causing economic losses and increased production time [15]. Also when wear occurs, the surface finish of parts is deficiency causing changes in the surfaces, this being a problem in these production processes making the coated material directly responsible for these problems [16]. One of the most used forms by industry for wear control is the application of protective coatings such as hard layers of carbides, nitrides, borides, oxides, etc., using techniques for depositing thin films [17].

This article was evaluated the coated steel 316LVM by physical deposition technique vapor state of nitrides of titanium and aluminum varying the percentage of these two elements, evidenced adequate performance of thin films when having major titanium content in the mixture.

2. EXPERIMENTAL PROCEDURE

$\text{Al}_x\text{Ti}_{1-x}\text{N}$ multilayer coatings have been grown onto AISI 316L steel substrates using a multi-target magnetron sputtering system, with an r.f. source (13.56 MHz) and two Al and Ti metallic targets with purity of 99.9%. The optima deposition parameters were the following: sputtering power of 350 W for Al and 400 W for the Ti target (these deposition parameters can generate a little non-homogeneous thickness of single layers due to the difference in the sputtering yield for Al and Ti materials); substrate temperature of 300°C; circular rotation substrate fixed to 60 RPM; an sputtering gas mixture of Ar 93% and N_2 7% under a total working pressure of $6 \cdot 10^{-3}$ mbar was employed. In this work the same nitrogen flow (3.7 sccm) was fixed for TiN and $\text{Al}_x\text{Ti}_{1-x}\text{N}$ ($\text{Al}_{0.3}\text{Ti}_{0.7}\text{N}$, $\text{Al}_{0.6}\text{Ti}_{0.4}\text{N}$ and $\text{Al}_{0.9}\text{Ti}_{0.1}\text{N}$) individual layers deposition with aim to analyze the substitution effect when the Al ions replace the Ti atoms. An unbalanced r.f. bias voltage, which generates a constant voltage offset of -70 V was applied. Moreover, the magnetron sputtering device has a positioning substrate system in relationship to target spot.

Fretting corrosion tests they were carried out in a galvanostat system for testing curves and electrochemical impedance spectroscopy on a Pin-on-disk system coupled to an electrochemical cell of three electrodes (Figure 1): A silver electrode silver (Ag / AgCl) chloride as a reference electrode, a platinum counter electrode and the sample as a working electrode, corrosive medium as Hanks` Balanced Salt Solution is used. Through the technique of Electrochemical Impedance Spectroscopy (EIS) with a 10 mV AC voltage, frequency range 300 kHz to 0.001 Hz, the polarization resistance and electrochemical behaviour was determined. The test parameters are shown in Table 1.

Table 1. Test Parameters

Sliding pattern	alumina balls
Diameter of ball	6 mm
Normal load	5 N
total sliding length	80 m
Velocity	4.7 cm/s

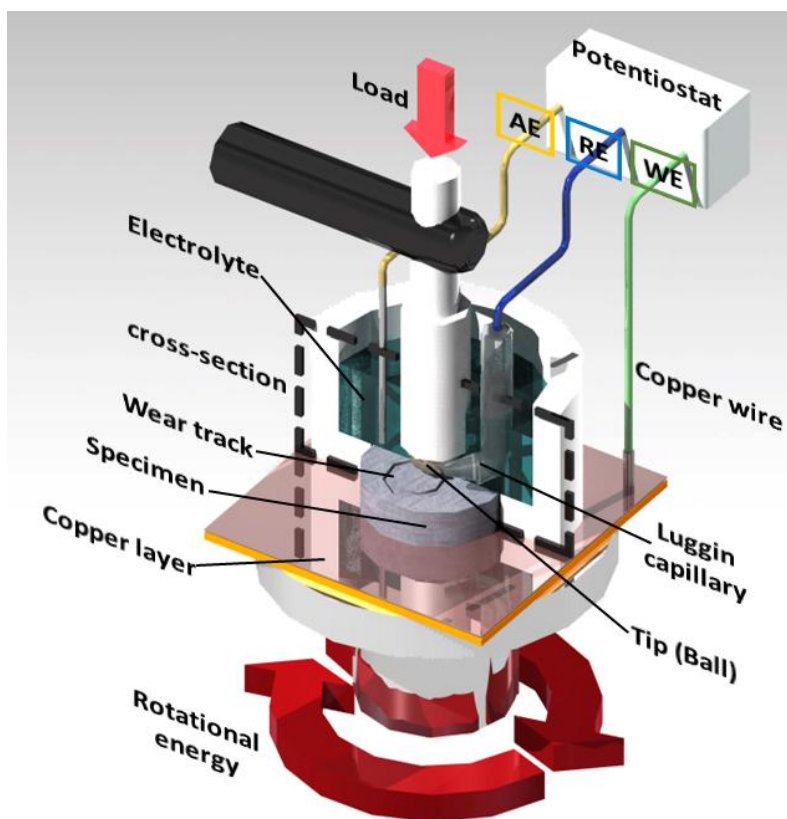


Figure 1. Schematic tribometer adequate equipment for corrosion wear tests [18]

To carry out this work, a team of X-ray X'pert Pro brand PANalytical with the following characteristics was used: copper anode tube wavelength = 1.54060 Å; a goniometer standard resolution containing the geometry (θ-θ) for performing measurements, symmetrical and asymmetrical and thin-film configurations minimum step size of 0.001 ° and a maximum of 1.27 °; proportional detector X-ray. To analyze the samples using diffraction techniques in Bragg-Brentano mode proper equipment

operation parameters were determined as the optimum angle of incidence ranging from 10° to 100° and the counting time of 1 second per step and the step size 0.03. For optimal angle of incidence diffractograms were made so thin film with a power of 45 kV and 40 mA. The database used ICDD for the identification and quantification of phases through X'Pert High Score software.

The surface characteristics, is determined with a JEOL scanning electron microscope. JSM-5000. Which is equipped with an electronic optics allow magnifications from 5X to 40.000X worked in high vacuum mode, It has a high sensitivity detector (multimode); for backscattered and secondary electrons.

3. RESULTS AND DISCUSSION

3.1 X-Ray Diffraction

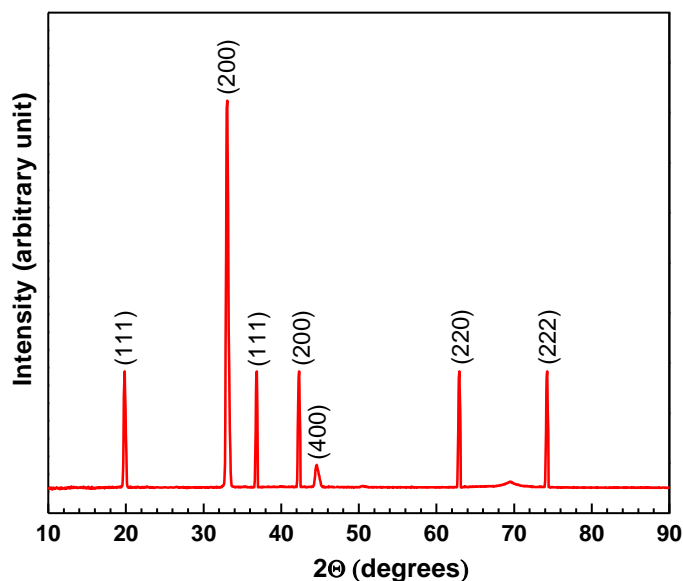


Figure 2. Pattern X-ray diffraction concerning the coating obtained by the PVD method on a steel substrate 316 LVM.

In Figure 2, the peaks of the diffractogram multilayer coating $\text{Al}_x\text{Ti}_{1-x}\text{N}$, is observed where the pattern presents a preferential orientation with Miller indices (200) associated with to cubic phase, since it corresponds to a composite material, it was necessary to perform a Rietveld refinement codes, other peaks of lesser magnitude correspond to the planes (222) (220) and (111) are associated with an FCC structure, the type of structure generated is substitutional type, where the Aluminum atoms entering the vacancies left by the Titanium, Nitrogen atoms are located in the cubic structure the form interstitial, attain to increase the packing factor, multilayer system generates a low residual stress, this is due to the effect of stress is reduced to interfaces that are characteristic of multilayer systems [19].

3.2 Scanning Electron Microscopy

In Figure 3, a micrograph obtained was observed by SEM one can observe the morphology of the coating which presents uniformity on the surface, smooth surfaces are evident, as the different variations micrographs of titanium and aluminum are similar, was selected micrograph corresponds to the film $\text{Al}_{0.3}\text{Ti}_{0.7}\text{N}$, the surface morphology of the coatings is strongly dependent on the type of substrate used coating growth is columnar [20]. The increase in grain size it is because the film growth it begins by forming a grain structure very small reflecting the initial density of nuclei. Since a layer obtained is continuous, the surface diffusion allows migration of atoms between neighboring grains, so that crystals incorporate lower surface energy more material and grow on adjacent crystals with higher surface energy, all this results in a dense network of columnar crystals.

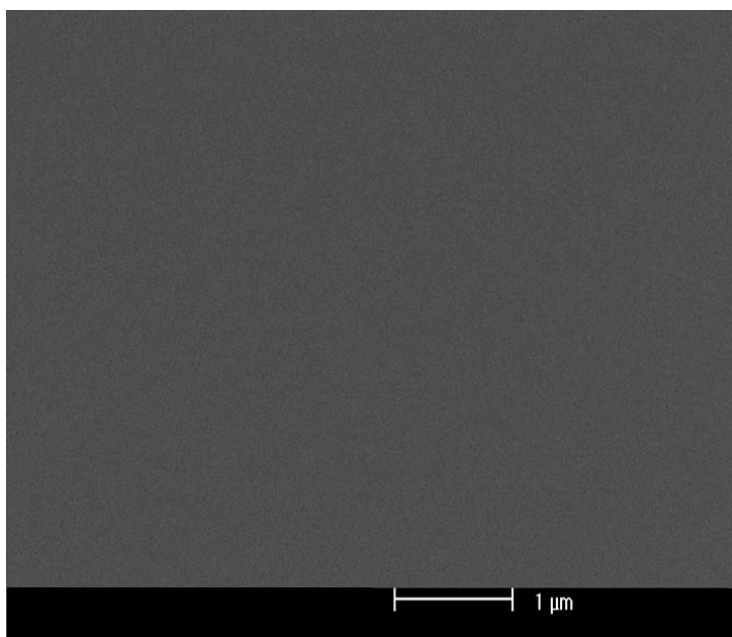


Figure 3. Image scanning electron microscopy $\text{Al}_{0.6}\text{Ti}_{0.4}\text{N}$ coating deposited on steel 316LVM.

3.3 Wear

Wear testing coating and the substrate steel AISI 316 L, they were conducted with the pin on disk type tribometer according to ASTM G99 standard. Figure 2, corresponding to the friction coefficient in function of distance. In each of the curves it shows that when starting occurs to test the coefficient of friction has increased because at this point the force of static friction is overcome between the two contact surfaces, but once initiated the relative movement of pin or counter-body (100Cr6 steel ball) on the uncoated surface and the friction coefficient decreases as the contact surfaces are deformed reaching a point which is approximately constant, that is, in this way, are formed and break bonds between the two surfaces and as the total number of these links varies, the coefficient is not constant. The behaviour shows the test conducted on the multilayer coating AlTiN

realizes the aforementioned fact only in this case the coefficient of friction has increased to a distance of approximately 15 meters, this is also due to the presence of free particles either the coating or the counter body at the point of contact of the two surfaces but then at distances greater than 20 m the coefficient tends to a value which is approximately constant. Additionally it demonstrated that contain a high amount of aluminum the coefficient is similar to that obtained with a high content of titanium,

Trends suggest curves the coefficient of friction increases for $\text{Al}_x\text{Ti}_{1-x}\text{N}$ on substrate steel 316LVM if the amount of titanium is equilibrated with respect to aluminum. In the case where higher concentration of titanium atoms in multilayers this ratio is generally superior to other mixtures, thus it is obtained a low roughness factor to increase the ratio of both titanium or aluminum, to find the lowest roughness factor corresponding to a balance of the two elements, This is because a homogeneous surface is achieved without agglomerations [21].

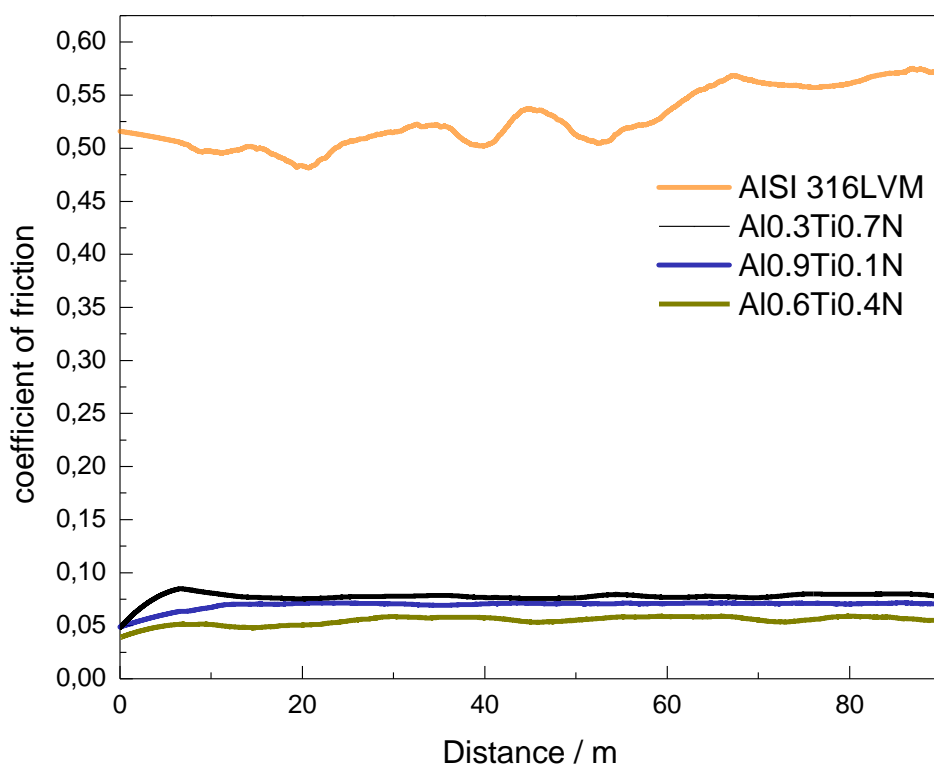


Figure 4. Coefficient of friction as a function of distance, for the multilayer coating of AlTiN and steel AISI 316L.

3.4 Tribocorrosion

Tribocorrosion tests consisted in synergistic assess wear and corrosion for this purpose the system shown in Figure 5 was used and it involves coupling of the electrochemical cell with Gamry PCI 4 device and pin-on-disk equipment, which allowed monitoring of corrosion and wear

simultaneously. To accomplish these tests the same parameters of the dry wear tests were used. This in order to compare the behavior against wear coatings with and without the presence of a corrosive environment in the figure 4, wear results are shown coating in the presence of a corrosive environment. According to the results obtained it can be seen that the coefficient of friction for multilayer AlTiN coatings, it is lower than reported by the uncoated steel because the friction coefficient also decreases. Behaviors can be seen that in the case of steel 316L the friction coefficient has a noticeable drop when it has traveled a distance of approximately 20 m, this drop occurs because as fluid is present small particles originated by the wear of the materials rapidly fall in contact with the two surfaces making is reduced for a few moments the direct contact between the pin and the steel surface 316 L.

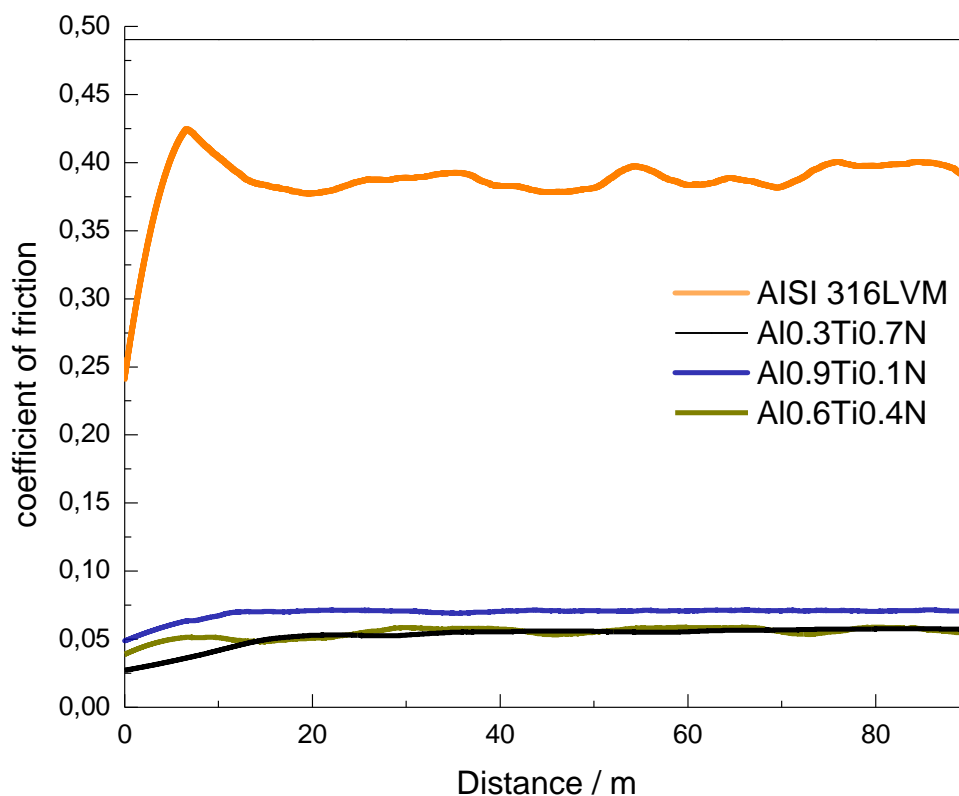


Figure 5. tribocorrosion behavior AlTiN multilayer coatings and 316L in the presence of a solution of 3.5% NaCl.

The behavior of the coatings against wear phenomena assisted by the electrochemical system creates adequate performance as the coefficient in all cases is decreased compared to wear in dry conditions, further the behavior of multilayer is different because systems with higher content of titanium generates less mechanical wear factor, because this element provides chemical stability and corrosion resistance, this is due to link atomically generated which has a higher binding energy to have a greater amount of titanium atoms which interact with this element wear and degradation mechanisms the two environments, indicating an improvement in the aspects of friction and wear, also chemical effects and biocompatibility, as these systems can work as functional coatings as improve the affinity

between the layers, basically becoming compatible in chemical bonds and create a decreased friction coefficients of material caused by the effect of the multilayer [22].

3.5 Electrochemical Impedance Spectroscopy

Before starting the test for determining the electrochemical degradation; the stabilized corrosion potential was measured in a period of 120 minutes then simultaneously the pin on disk and potentiostat were activated. In Figure 6 Nyquist plots obtained for the coatings and the substrate are shown an increase of the total impedance for the coating because the resistance value increases this indicates that the protective effect of the coating is excellent and improves the performance found in multilayer systems due to the effect of obtained multilayer. After analyzing the curves, it can be seen that the polarization resistance for coatings is higher compared to that reported for the substrate, indicating a decrease in corrosion rate.

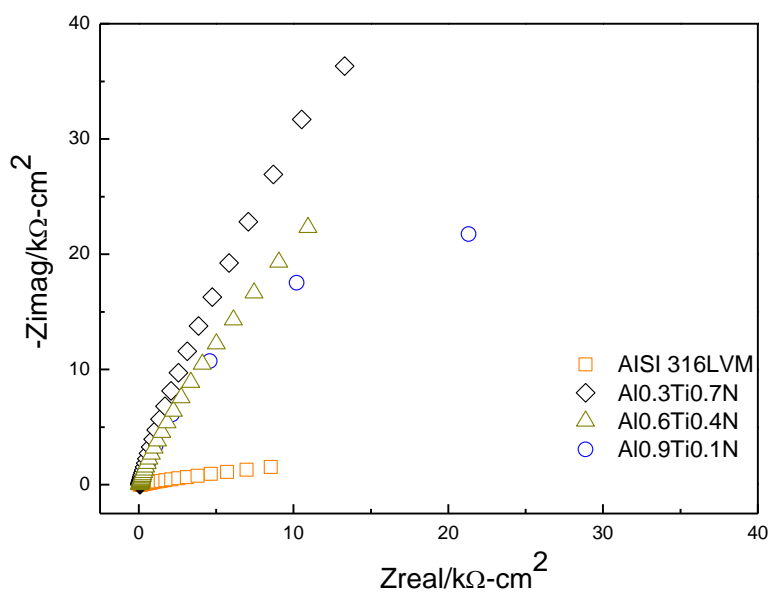


Figure 6. Nyquist diagrams for multilayer coatings and steel AISI 316L, subject to tribocorrosion.

The electrochemical response to determine the phenomena generated in the interface of the coating that model through circuits having two constant phase elements and was performed the simulation of the experimental data. In evaluating the impedance of each of the systems, it can be argued that in the instant the value of the imaginary part tends to zero, the polarization resistance (R_p) becomes equal to the value of resistivity, making it possible to indicate that in saline, Hank the material with higher content of titanium ($Al_{0.3}Ti_{0.7}N$) has the higher polarization resistance values, followed by the sample ($Al_{0.6}Ti_{0.4}N$), continuing with ($Al_{0.9}Ti_{0.1}N$) and lastly the uncoated sample, this may be denoted as the intercept on the ordinate axis increases in proportion to the value of current density.

The trend indicates that to generate the coating are increases the resistance to polarization compared to the uncoated alloy, addition, as the titanium content in the mixture increases the value of current density it decreases so that the material is protected to a greater extent as shown in Figure 6.

According to the electrochemical reaction it is stressed that the multilayers with a high content of titanium, they are displaced towards protection zone, but nevertheless there is no direct relationship with the increase in the percentage of aluminum. Since accelerated generating electroless solution for steel 316LVM increase is observed, this change can be distinguished as the start of the formation of a corrosion resistance stably due to a further increase in impedance.

4. CONCLUSIONS

The multilayer coatings confer industrial steel AISI 316L advantageous resistance to polarization and a lower corrosion rate ensuring their use in mechanical systems exposed to tribocorrosion phenomena.

When comparing the results of wear, corrosion and tribocorrosion (synergy between corrosion - wear) multilayer coatings for the dry wear was observed that the friction coefficient decreases in comparison with the substrate, tribocorrosion results showed a coefficient of less than reported in dry wear for the two cases studied friction.

The multilayer titanium aluminum nitride have good tribological performance (low friction). Obtaining combined properties as coefficient of friction and corrosion resistance generate a possible application of biocompatibility.

ACKNOWLEDGEMENTS

Thanks the financial support from the Universidad Militar Nueva Granada, contract number ING-1903-2015.

References

1. N. Reckinger, C.A. Duțu, X. Tang, E. Dubois, D.A. Yarekha, S. Godey, L. Nougaret, A. Łaszcz, J. Ratajczak, J.-P. Raskin, *Thin Solid Films*, 520 (2012) 4501
2. R.R. Krishnan, K.G. Gopchandran, V.P. Mahadevan Pillai, V. Ganesan, Vasant Sathe, *Appl. Surf. Sci.*, 255 (2009) 7126
3. F.F. Yang, L. Fang, S.F. Zhang, J.S. Sun, Q.T. Xu, S.Y. Wu, J.X. Dong, C.Y. Kong, *Appl. Surf. Sci.*, 254 (2008) 5481
4. M.P. Suryawanshi, S.W. Shin, U.V. Ghorpade, K.V. Gurav, C.W. Hong, G.L. Agawane, S.A. Vanalakar, J.H. Moon, Jae Ho Yun, P.S. Patil, Jin Hyeok Kim, A.V. Moholkar, *Electrochim. Acta.*, 150 (2014) 136
5. Y. P. Yang, M.-Show Wong, *Surf. Coat. Technol.*, 259 (2014) 129
6. D. Prieling, H. Steiner, *Int. J. Heat Mass Transfer*, 65 (2013) 10
7. S. Krischok, A. Ulbrich, T. Ikari, V. Kempter, M. Marschewski, O. Höfft, *Nucl. Instrum. Methods Phys. Res., Sect. B*, 340 (2014) 51

8. A. Metel, V. Bolbukov, M. Volosova, S. Grigoriev, Yu. Melnik, *Surf. Coat. Technol.*, 225 (2013) 34
9. T.Q. Dong, V.V. Hoang, G. Lauriat, *Thin Solid Films*, 545 (2013) 584
10. M.F. Meléndrez, F. Solis-Pomar, C.D. Gutierrez-Lazos, P. Flores, A.F. Jaramillo, A. Fundora, E. Pérez-Tijerina, *Ceram. Int.*, 42 (2016) 1160
11. D. Batory, A. Jdrzejczak, W. Szymanski, P. Niedzielski, M. Fijalkowski, P. Louda, I. Kotela, M. Hromadka, J. Musil, *Thin Solid Films*, 590 (2015) 299
12. M. Zhou, S. Roualdès, J. Zhao, V. Autès, A. Ayrat, *Thin Solid Films*, 589 (2015) 770
13. N. Zotov, S. Baumann, W.A. Meulenber, R. Vaßen, *J. Membr. Sci.*, 442 (2013) 119.
14. B. J. Lee, S. C. Cho, G. H. Jeong, *Curr. Appl Phys.*, 15 (2015) 563.
15. K. Moerlooze, F. Al-Bender, H. V. Brussel, *Wear* 271 (2011) 1005
16. V. G. Pina, A. Dalmau, F. Devesa, V. Amigó, A. I. Muñoz, *J. Mech. Behav. Biomed. Mater.*, 46 (2015) 59
17. R. Bayón, A. Igartua, J.J. González, U. Ruiz de Gopegui, *Tribol. Int.*, 88 (2015) 115
18. W. Aperador, A. Delgado, E. Vera, *Int. J. Electrochem. Sci.*, 10 (2015) 4473
19. Q. Feng, T. Li, H. Teng, X. Zhang, Y. Zhang, C. Liu, Junze Jin, *Surf. Coat. Technol.*, 202 (2008) 4137
20. R. Krishna, G. Poshal, A. Jyothirmayi, G. Sundararajan, *Mater. Des.*, 77, , 6-14, 2015.
21. J. Jiang, Q. Zhou, J. Yu, A. Ma, D. Song, F. Lu, L. Zhang, D. Yang, J. Chen, *Surf. Coat. Technol.*, 216 (2013) 259
22. H. Zhao, S. Cai, S. Niu, R. Zhang, X. Wu, G. Xu, Z. Ding, *Ceram. Int.*, 41 (2015) 4590
23. K. Kilan, P. Warszyński, *Electrochim Acta*, 144 (2014) 254
24. D. Rafaja, C. Schimpf, T. Schucknecht, V. Klemm, L. Péter, I. Bakonyi, *Acta Mater*, 59 (2011) 2992
25. N.E. Beliardouh, K. Bouzid, C. Nouveau, B. Tlili, M.J. Walock, *Tribol Int*, 82 (2015) 443